Fig. 11. Quality factor variations of the SDR for TM_{101} mode.

the TE_{101} mode (effectively, here, the resonant frequency of the shielded dielectric resonator on the TE_{102} mode follows the variation of the resonant frequency of metallic cavity on the TE_{101} mode).

The second Q plateau ($7 < b < 10$) corresponds to the inverse of the loss tangent of the dielectric material on the TE_{101} mode.

The last increase converges to the Q values of the metallic cavity on the TE_{102} mode (the frequency follows here, the one of metallic cavity on TE_{101} mode).

ACKNOWLEDGMENT

We thank D. Kajfez for his valuable comments.

REFERENCES

- [1] J. Broc, "On the characteristics of electromagnetic resonant cavities formed by two concentric spheres," *C. R. Acad. Sei. (Paris)*, vol. 230, pp. 198-200, 1950.
- [2] H. Y. Yee, "An investigation of microwave dielectric resonators," M. L. Rep. No. 1065, Stanford Univ., July 1963.
- [3] M. Gastine, "Résonances électromagnétiques d'échantillons diélectriques," Thèse de docteur 3^e cycle, Faculté des Sciences d'Orsay, 1967.
- [4] P. Affolter, Eliasson, "Electromagnetic resonances and Q -factor of lossy dielectric spheres," *IEEE*, no. 9, Sept. 1973.
- [5] P. Affolter, A. Käch, "Resonance frequencies of a dielectric sphere contained within a concentric shield," *Arch. Elektr. Übertragungstechn.* (AEÜ), vol. 27, no. 10, pp. 423-432, (in German).
- [6] I. Wolff, H. Hofmann, "The three-layer sphere resonator," *Frequenz*, vol. 27, no. 5, pp. 110-119, 1973, (in German).
- [7] I. Wolff, N. Schwab, "Measurement of the dielectric constant of anisotropic dielectric materials, using the degenerated modes of a spherical cavity," in *Proc. 10th Euro. Microwave Conf.*, (Warszaw) 1980, pp. 241-245.
- [8] NTK: Technical Ceramics Division, NGK spark plugs-Catalog

Accurate Approach for Computing Quasi-Static Parameters of Symmetrical Broadside-Coupled Microstrips in Multilayered Anisotropic Dielectrics

MANUEL HORN, MEMBER, IEEE, AND FRANCISCO MEDINA

Abstract — In this paper, we present a method for calculating the propagation parameters of shielded broadside- and broadside edge-coupled microstrips in multilayered anisotropic dielectrics.

Manuscript received August 8, 1985; revised January 23, 1986. This work was supported in part by the Comisión Asesora de Investigación Científica y Técnica, Spain.

The authors are with the Departamento de Electricidad y Electrónica, Facultad de Física, Universidad de Sevilla, 41012, Seville, Spain.

IEEE Log Number 8607967.

crostrip transmission lines. Conductor strips are assumed to be embedded in a multilayered isotropic and/or anisotropic medium. This method provides accurate expressions for computing upper and lower bounds for the true values of mode capacitances. The effects of side wall-shielding and anisotropy of the material are investigated. Some particular multilayered structures are analyzed, which could be applied to the design of directional couplers and filters.

I. INTRODUCTION

As is well known, coupled lines are extensively used as building blocks for a great variety of microwave circuit components for communication systems [1]-[3]. The electrical response of coupled line systems has been studied using the ABCD or impedance matrix formulation [4], [5], and these techniques require prior knowledge of the mode characteristic impedances and phase velocities of the structure to be used. When weak coupling must be achieved, edge-coupled strips on a dielectric substrate are widely used. This configuration yields small deviations from equal mode-phase velocities, but these can be suppressed by using adequate techniques [6], [7]. However, if a strong coupling is needed, broadside-coupled configurations are more adequate. If the strips are embedded in an inhomogeneous and/or anisotropic dielectric medium, deviations from equality of phase velocities appear. In fact, large phase velocity ratios can be achieved with broadside-coupled structures, which is useful for the design of single section components with complex electrical responses [8]. Nevertheless, if equal mode-phase velocities are required, matching can be achieved if we use multiedielectric iso/anisotropic configurations.

Broadside-coupled and broadside edge-coupled structures have been studied by several authors using different methods [8]-[15]. The purpose of this paper is to present a unified formulation to analyze these configurations, in a multilayered iso/anisotropic medium. The multiple boundaries problem is treated by using a variational method in the spectral domain. The application of this method provides two numerically efficient algorithms that yield upper and lower bounds for the exact values of the mode capacitances for this type of transmission lines. We have applied the method to several particular cases, and also reported the influence of the side walls and anisotropy.

II. ANALYSIS

The cross sections of the structures that are the object of this study are represented in Fig. 1. For both configurations we will assume perfect conductors and lossless dielectric layers. We will also assume strips with valueless thickness. The electrical permittivity of the i -th dielectric layer is given by the following diagonal tensor:

$$\bar{\epsilon}_i = \epsilon_o \begin{bmatrix} \epsilon_x^i & 0 \\ 0 & \epsilon_y^i \end{bmatrix}, \quad i = 1, \dots, N. \quad (1)$$

Although the inhomogeneous nature of the dielectric medium precludes pure TEM-mode propagation, one can use the quasi-TEM approximation as long as the cross-sectional dimensions are much smaller than the wavelength. In this case, structures in Fig. 1(a) and (b) can support two and four orthogonal modes of propagation, respectively. By determining each mode capacitance, we can in turn discover the electrical behavior of the coupled transmission line. To evaluate the mode capacitances, one can simplify the problem by taking into account the symmetry of the structure. In fact, we only need analyze one quadrant of the cross section shown in Fig. 1(a) or (b) (the upper right

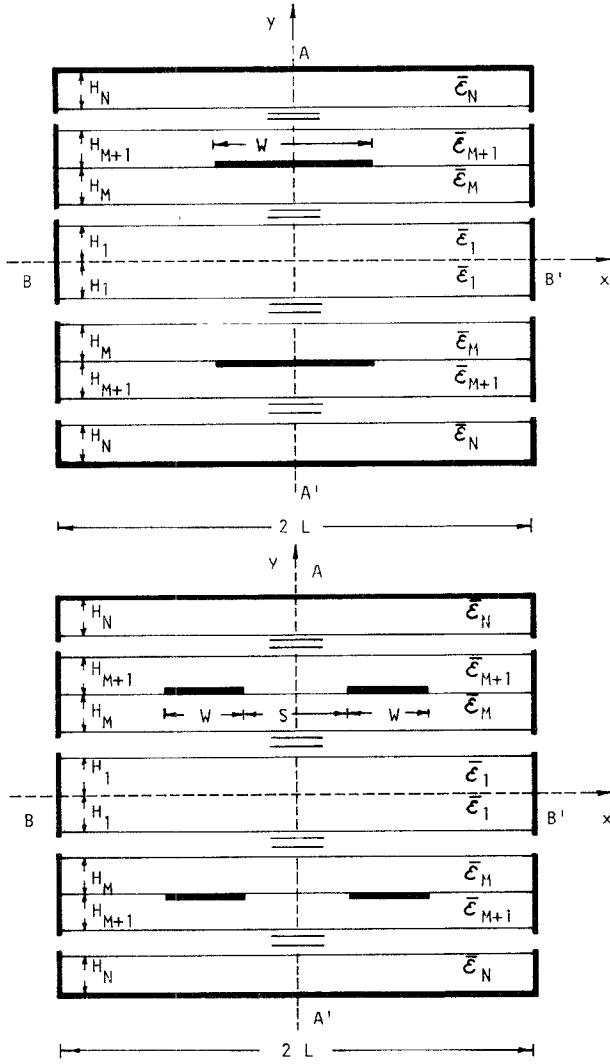


Fig. 1. Cross sections of (a) broadside-coupled, and (b) broadside edge-coupled strips embedded in a multilayered iso/anisotropic dielectric medium.

quarter, for instance) and assume the planes of symmetry AA' and BB' to be electric and/or magnetic walls. Thus, the modes for the structure in Fig. 1(a) are

- a) even mode (*e*): AA' and BB' magnetic walls.
- b) odd mode (*o*): AA' magnetic wall, BB' electric wall.

For the configuration in Fig. 1(b) they are

- a) even-even (*ee*): AA' and BB' magnetic walls.
- b) even-odd (*eo*): AA' magnetic wall, BB' electric wall.
- c) odd-even (*oe*): AA' electric wall, BB' magnetic wall.
- d) odd-odd (*oo*): AA' and BB' electric walls.

The characteristic impedances (Z_o^m) and phase velocities (V_{ph}^m) for each mode are obtained from the capacitances of the structure filled with dielectric (C_d^m), and air (C_a^m) in the following way:

$$Z_o^m = \frac{120\pi\epsilon_o}{\sqrt{C_d^m \cdot C_a^m}} \quad (2)$$

$$V_{ph}^m = c\sqrt{C_a^m/C_d^m}, \quad m = e, o, ee, eo, oe, oo \quad (3)$$

where c is the velocity of light in free space and m refers to the mode.

In this paper, we use the variational method in the spectral domain to evaluate the mode capacitances, writing them as functions of surface charge density or potential at the M th

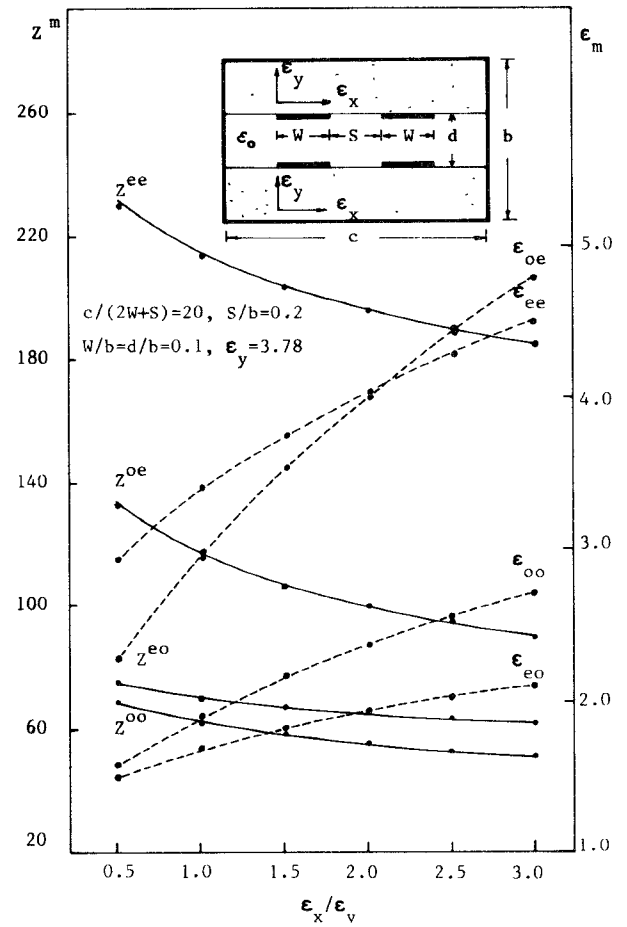


Fig. 2. Mode characteristics impedances (Z^{ee} , Z^{eo} , Z^{oe} , Z^{oo}) and effective dielectric constants (ϵ_{ee} , ϵ_{eo} , ϵ_{oe} , ϵ_{oo}) versus anisotropy ratio (ϵ_x/ϵ_y) of the dielectric substrate for broadside edge-coupled microstrip. This graphic is reported by S. K. Koul and B. Bhat in [14]. The black dots have been calculated by using the method in this paper.

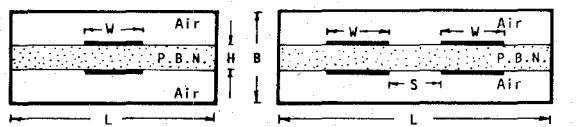
interface (see Fig. 1) in the following way:

$$C_m = (1/2pLV^2) \sum_{n=1}^{\infty} \tilde{L}_M(n) \cdot |\tilde{V}_M^m(n)|^2 \quad (4a)$$

$$C_m^{-1} = (1/2pLQ^2) \sum_{n=1}^{\infty} \tilde{G}_M(n) \cdot |\tilde{p}_M^m(n)|^2 \quad (4b)$$

$m = e, o, ee, eo, oe, oo$, $p = 1$ for broadside-coupled strips, $p = 2$ for broadside edge-coupled strips, Q and V are the charge and the potential of the strips, respectively, $\tilde{V}_M^m(n)$ and $\tilde{p}_M^m(n)$ the discrete Fourier transforms of the potential and surface charge density at the interface where the strips are located (M th), and $\tilde{G}_M(n) = \{\tilde{L}_M(n)\}^{-1}$ the spectral Green's function for the problem. As stated in [16], the definition of the Fourier transform must take into account the boundary conditions at the vertical side walls. Green's function is determined following the method reported by the authors in [16], but a simplified recurrence formula for $\tilde{L}_M(n)$ (accounting for the symmetry of the configurations) is offered in Appendix I. The expressions (4a) and (4b) are stationary, and provide very accurate results if appropriate trial functions to approximate $\rho_M^m(x)$ or $V_M^m(x)$ are chosen. In this paper, trial functions are expanded in a set of basis functions, and the coefficients of such expansion are determined using the Rayleigh-Ritz's optimization procedure. We obtain very accurate results with the trial functions in the Appendix of [16], taking only one or two terms for the charge density expansion,

TABLE I
COMPARISON OF THE RESULTS OBTAINED FROM THE UPPER (UB)
AND LOWER BOUND (LB) ALGORITHMS FOR SEVERAL
SHAPE RATIOS



W/H	Z_o	Z_e	S/H	Z_{eo}	Z_{oo}	Z_{ee}	Z_{oe}	ALG.
.25	100.5	239.3	.5	116.6	83.79	374.6	99.53	L.B.
	99.90	238.5		116.4	83.16	371.6	99.42	U.B.
1.0	52.15	182.6	.2	61.69	39.43	285.9	56.42	L.B.
	52.09	181.2		61.69	39.42	283.8	56.39	U.B.

$L/H = 10$; $B/H = 6$; $\epsilon_x = 5.12$; $\epsilon_y = 3.40$ (P.B.N.)

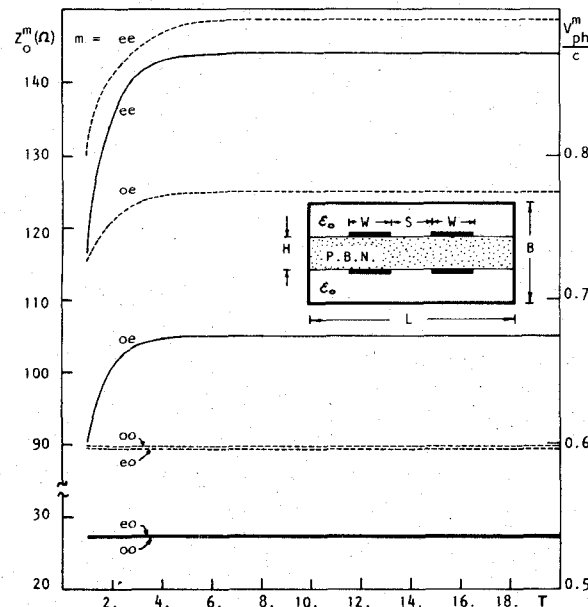


Fig. 3. Influence of the vertical side walls on mode parameters for broadside edge-coupled strips on PBN substrate ($\epsilon_x = 5.12$, $\epsilon_y = 3.40$). The independent variable is $T = L - W - S$. $B/H = 5$ and $W/H = S/H = 2.5$. — mode impedances (Z_o^m). - - - normalized phase velocities (V_{ph}^m/c).

and three or four for the potential expansion. It must be emphasized that numerical data computed using (4a) and (4b) are, respectively, upper and lower bounds for the exact values of the mode capacitances. Thus, we can determine a margin of error for the results and improve their reliability.

III. NUMERICAL RESULTS

Before obtaining reliable results, we checked the accuracy of the method in this paper with previously reported graphic data [10], [11], [13]–[15], and a good agreement was found (for example, see Fig. 2). Moreover, upper (UB) and lower bound (LB) algorithms have been used simultaneously to improve the reliability of the computed data. In Table I, a comparison of the numerical results obtained from both algorithms is shown. Discrepancy is less than 1 percent. Nevertheless, it has been proven that the LB algorithm is numerically more efficient than the UB one for this type of structure, since trial functions for charge density are more adequate. This is why the LB algorithm has been used to compute the graphic design data shown here.

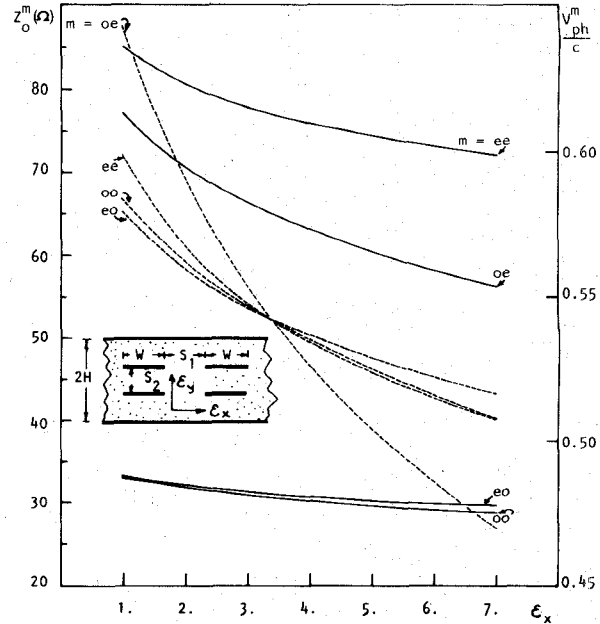


Fig. 4. Influence of the anisotropy on the propagation parameters of a broadside edge-coupled structure (ϵ_x varying from 1 to 7 and ϵ_y having a fixed value $\epsilon_y = 3.40$). $S_1/H = W/H = 1.0$ and $S_2/H = 0.6$. — mode impedances (Z_o^m). - - - normalized phase velocities (V_{ph}^m/c).

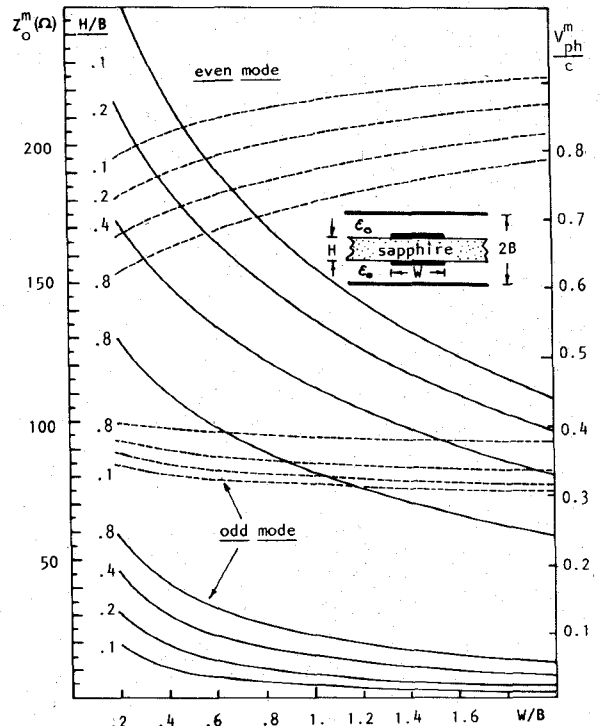


Fig. 5. Characteristic parameters of a broadside-coupled configuration on sapphire substrate ($\epsilon_x = 9.40$, $\epsilon_y = 11.60$) versus W/B for several values of H/B . — mode impedances (Z_o^m). - - - normalized phase velocities (V_{ph}^m/c).

The effect of the vertical side walls on propagation parameters is shown in Fig. 3. It can be seen that even-even and odd-odd modes are much more affected than even-odd and odd-even ones, as should be expected from each mode-field distribution. In any case, if $L/B > 10$ or 15, for example, this effect can be neglected. Thus, by sufficiently enlarging L/B , open structures can also be analyzed.

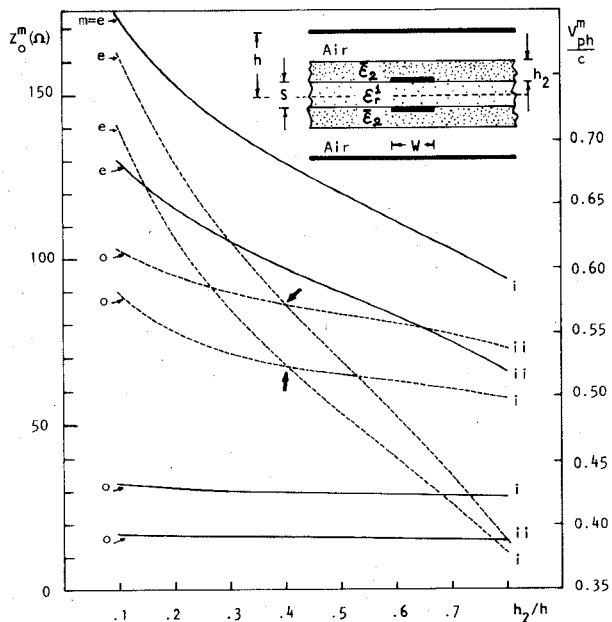


Fig. 6. Propagation parameters of broadside-coupled strips with dielectric overlay varying the h_2/h ratio. Matching points for phase velocities are marked with arrows. $S/h = 0.20$; $\epsilon_x^1 = 2.50$ and $\epsilon_x^2 = 9.40$, $\epsilon_y^2 = 11.60$. (i) $W/h = 0.40$; (ii) $W/h = 1.0$. — mode impedances (Z_o^m). - - - normalized phase velocities (V_{ph}^m/c).

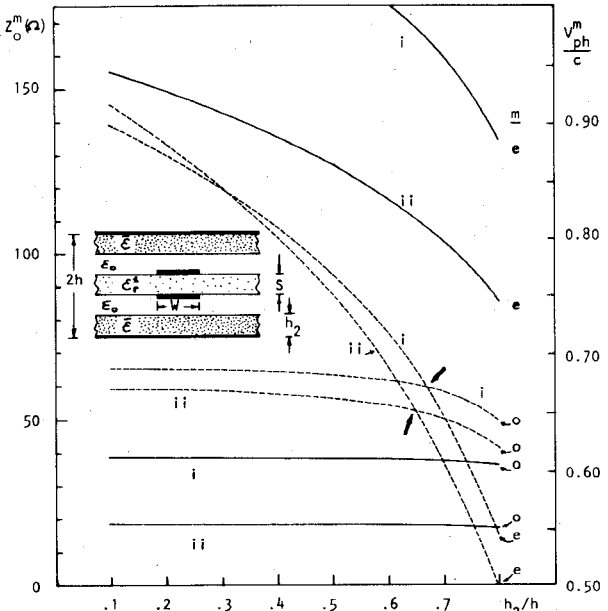


Fig. 8. Alternative structure to the configuration in Fig. 6. Dimensions, materials, and notation are the same as in Fig. 6.

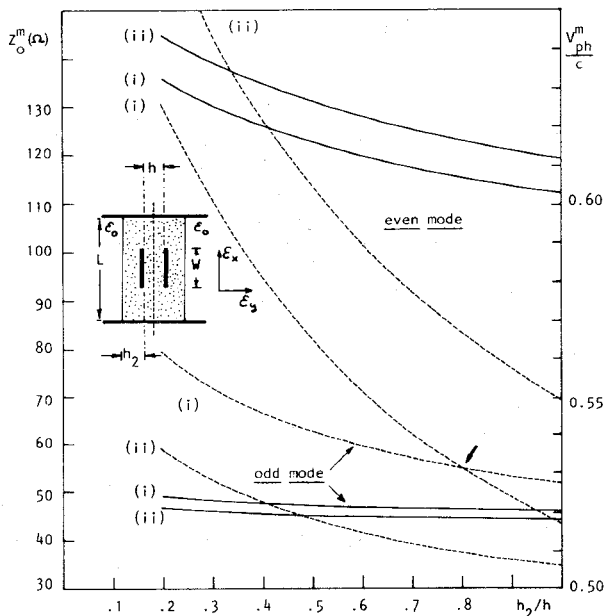


Fig. 7. Broadside-coupled strips embedded in (i) PBN ($\epsilon_x = 5.12$, $\epsilon_y = 3.40$). (ii) an isotropic dielectric with $\epsilon_r = 4.1$ ($\approx \sqrt{\epsilon_x \epsilon_y}$). Varying h_2/h , mode-phase velocities can be matched in case (i), but this is not possible in case (ii). $W/h = 1.0$ and $L/h = 5.0$. — mode impedances (Z_o^m). - - - normalized phase velocities (V_{ph}^m/c).

Fig. 4 shows the effect of the anisotropy of the dielectric material on the characteristic parameters. Although the structure is homogeneous, mode-phase velocities are different in a significant amount. The curves for normalized phase velocities coincide when $\epsilon_x = \epsilon_y$, that is, in the isotropic case.

In Fig. 5, we show a set of design graphics for broadside-coupled strips on sapphire substrate. It can clearly be seen that large phase velocity ratios are possible with this dielectric material.

This fact is useful in certain coupler and filter applications. However, in coupler design, phase velocity matching is normally needed. Fig. 6 shows an overlay configuration for achieving equal mode-phase velocities: using a superstrate with high dielectric constant (compared with the dielectric constant of the substrate), it is possible to match the phase velocities, although coupling is decreased. Fig. 7 shows another configuration which allows us to obtain equal phase velocities using only one anisotropic dielectric material such as pyrolytic boron nitride. We can also see that this is not possible with isotropic materials.

The performance of the overlay coupler is very sensitive to the presence of air bubbles between the dielectric layers. This problem can be avoided by using the configuration in Fig. 8. In this structure, odd-mode parameters remain unaffected by the high-permittivity dielectric layer, and even-mode parameters can be tuned by varying the thickness of such layer. High-directivity directional couplers with tight coupling could be designed using these configurations.

IV. CONCLUSIONS

A variational method in the spectral domain has been used for obtaining two useful computational algorithms to determine upper and lower bounds for mode capacitances of shielded broadside-coupled and broadside edge-coupled microstrip or striplines embedded in a layered iso/anisotropic substrate medium. Both algorithms yield accurate results and so their reliability is guaranteed. We have seen that side wall-shielding significantly affects the even, odd-even, and even-even modes, while odd, odd-odd, and even-odd modes remain practically unchanged (except, obviously, if the side walls are very close to the strips). The anisotropy of the dielectric medium also has been investigated, and shown to significantly affect the propagation parameters. However, it is possible to take advantage of such anisotropy in some special configurations. Several iso/anisotropic structures, which allow us to match mode-phase velocities, have also been studied. These structures could be applied to directional coupler design.

APPENDIX I
RECURRENCE EXPRESSION TO EVALUATE THE
GREEN'S FUNCTION

In this Appendix, we present a recurrence formula to evaluate $\tilde{L}_M(n)$. (M is the number of the interface with conductor strips and n is the number of dielectric layers.)

$$\tilde{L}_M(n) = \tilde{L}'_M(n) + \tilde{L}''_{N-M}(n) - \tilde{g}_{M,M}(n) \quad (A1)$$

with

$$\tilde{L}'_i(n) = \tilde{g}_{i,i}(n) - \frac{\tilde{g}_{i-1,1}^2(n)}{\tilde{L}'_{i-1}(n)} \quad (A2a)$$

$$\tilde{L}''_i(n) = \tilde{g}_{N-i,N-i}(n) - \frac{\tilde{g}_{N-i,N-i+1}^2(n)}{\tilde{L}''_{i-1}(n)}, \quad i = 2, \dots, N-1. \quad (A2b)$$

The boundary conditions at lower and upper interfaces for each mode are taken into account by $L'_1(n)$ and $L''_1(n)$ in the following way:

$$\tilde{L}'_1(n) = \tilde{g}_{1,1}(n) - 2pk_n\epsilon_{eq}^1 \cdot \{ \sinh(2k_n H_{eq}^1) \}^{-1} \quad (A3a)$$

$$\tilde{L}''_1(n) = \tilde{g}_{N-1,N-1}(n), \quad (A3b)$$

$p = 0$ for odd, even-odd, and odd-odd modes, $p = 1$ for even, even-even, and odd-even modes, k_n is the discrete Fourier variable, and the equivalent heights and permittivities are given by

$$\epsilon_{eq}^i = \sqrt{\epsilon_x^i \cdot \epsilon_y^i} \quad (A4a)$$

$$H_{eq}^i = H_i \cdot \sqrt{\epsilon_x^i / \epsilon_y^i}. \quad (A4b)$$

The $\tilde{g}_{i,i}(n)$ are defined as follows:

$$\tilde{g}_{i+1,i}(n) = \tilde{g}_{i,i+1} = -\epsilon_o k_n \epsilon_{eq}^{i+1} \{ \sinh(k_n H_{eq}^{i+1}) \}^{-1} \quad (A5a)$$

$$\tilde{g}_{i,i}(n) = \epsilon_o k_n \{ \epsilon_{eq}^{i+1} \coth(k_n H_{eq}^{i+1}) + \epsilon_{eq}^i \coth(k_n H_{eq}^i) \}. \quad (A5b)$$

These expressions are easily evaluated in a digital computer and we can write a subroutine program which considers as inputs the number of dielectric layers and their thickness and permittivity, and provides as output the corresponding Green's function in the spectral domain ($\tilde{G}_M(n) = \tilde{L}_M(n)^{-1}$). Thus, the complexity of the dielectric medium is no longer a difficulty.

REFERENCES

- [1] G. Matthaei, L. Young, and E. M. T. Jones, *Microwave Filters, Impedance-Matching Networks, and Coupling Structures*, Dedham MA: Artech House, 1980.
- [2] S. Frankel, *Multiconductor Transmission Line Analysis*. Dedham, MA: Artech House, 1977.
- [3] Y. Tajima and S. Kamihashi, "Multiconductor couplers," *IEEE Trans. Microwave Theory Tech.*, vol. MTT-28, pp. 529-535, June 1980.
- [4] J. L. Allen, "Nonsymmetrical-coupled lines in an inhomogeneous dielectric medium," *Int. J. Electron.*, vol. 38, no. 3, pp. 337-347, Mar. 1975.
- [5] V. K. Tripathi, "Asymmetric-coupled transmission lines in an inhomogeneous medium," *IEEE Trans. Microwave Theory Tech.*, vol. MTT-23, pp. 734-739, Sept. 1975.
- [6] D. D. Paolino, "MIC overlay coupler design using spectral domain techniques," *IEEE Trans. Microwave Theory Tech.*, vol. MTT-26, pp. 646-649, Sept. 1978.
- [7] M. Horro and R. Marques, "Coupled microstrips on double anisotropic layers," *IEEE Trans. Microwave Theory Tech.*, vol. MTT-32, pp. 467-471, Apr. 1984.
- [8] W. J. Barnes and J. L. Allen, "Modified broadside-coupled strips in a layered dielectric medium," *Int. J. Electron.*, vol. 40, no. 4, pp. 377-391, Apr. 1976.

- [9] R. Crampagne, B. Mangin, and J. David, "Dispersion characteristics of superimposed microstrip couplers," *Int. J. Electron.*, vol. 42, pp. 479-484, May 1977.
- [10] I. J. Bahl and P. Bhartia, "Characteristics of inhomogeneous broadside-coupled striplines," *IEEE Trans. Microwave Theory Tech.*, vol. MTT-28, pp. 529-535, June 1980.
- [11] A. D'Assuncao, A. Giarola, and D. Rogers, "Characteristics of broadside-coupled microstrip lines with iso/anisotropic substrates," *Electron. Lett.*, vol. 17, no. 7, pp. 264-265, 1981.
- [12] I. J. Bahl and P. Bhartia, "The design of broadside-coupled stripline circuits," *IEEE Trans. Microwave Theory Tech.*, vol. MTT-29, pp. 165-168, Feb. 1981.
- [13] S. K. Koul and B. Bhat, "Broadside edge-coupled symmetric strip transmission lines," *IEEE Trans. Microwave Theory Tech.*, vol. MTT-30, pp. 1874-1880, Nov. 1982.
- [14] S. K. Koul and B. Bhat, "Generalized analysis of microstrip-like transmission lines and coplanar strips with anisotropic substrates for MIC, electrooptic modulator, and SAW application," *IEEE Trans. Microwave Theory Tech.*, vol. MTT-31, pp. 1051-1058, Dec. 1983.
- [15] S. K. Koul and B. Bhat, "A generalized TEM analysis of broadside-coupled planar transmission lines with isotropic and anisotropic substrates," *AEU*, vol. 38, no. 1, pp. 37-45, Jan./Feb. 1984.
- [16] F. Medina and M. Horro, "Upper and lower bounds on mode capacitances for a large class of anisotropic multilayered microstrip-like transmission lines," *IEE Proc. Microwave, Opt. Antennas*, pt. H, vol. 132, no. 3, pp. 157-163, June 1985.

Faster Computation of Z -Matrices for Rectangular Segments in Planar Microstrip Circuits

ABDELAZIZ BENALLA AND K. C. GUPTA

Abstract—Currently available formulation of Z -matrices for rectangular segments in planar microstrip circuits involves numerical summation of the doubly infinite series in the corresponding Green's function. These computations can be accelerated considerably by using the formulation proposed here which is based on an analytical treatment of one of the summations involved.

I. INTRODUCTION

The planar circuit approach (or two-dimensional circuit approach) has been used for characterization of microstrip components [1]–[5] as well as microstrip antennas [6]–[9]. Microstrip circuits may be treated as planar two-dimensional circuits by using the planar waveguide model [10] for microstrip lines. Segmentation [4], [11] and desegmentation methods [12] used for two-dimensional circuit analysis involve computations of Z -matrices for various planar segments in the circuit. Most common circuit segments have rectangular shapes and the Z -matrix for a rectangular segment is obtained [1], [13] by using a two-dimensional impedance Green's function, which is available as a doubly infinite series involving various modes along the two edges of the rectangular segment. Consequently, computations of Z -matrices based on the currently available formulas [1], [13] involve numerical summation of a doubly infinite series. Because of the slow convergence of these series, a large number of terms (typically 100×100) is needed to obtain sufficiently accurate results. This

Manuscript received August 19, 1985; revised January 3, 1986. This work was supported in part by the Office of Naval Research under Contract N00014-84-K-0349.

The authors are with the Department of Electrical and Computer Engineering, University of Colorado, Boulder, CO 80309.

IEEE Log Number 8607979.